Parameterization of Net All-Wave Radiation for Urban Areas

B. OFFERLE AND C. S. B. GRIMMOND

Indiana University, Bloomington, Indiana

T. R. OKE

University of British Columbia, Vancouver, British Columbia, Canada

ABSTRACT

A simple scheme to estimate net all-wave radiation ($Q*$) is evaluated using annual datasets in three urban settings (Chicago, Illinois; Los Angeles, California; and Łódź, Poland). Results are compared with a regression model based on incoming solar radiation and with an urban canopy-layer model incorporating a canyon geometry radiation scheme that requires a larger set of meteorological and surface property inputs. This net all-wave radiation parameterization (NARP) is most sensitive to albedo and the effects of clouds on incoming longwave radiation. Although omitting the diurnal variation of albedo has little impact on overall model fit, its seasonal variability needs to be considered in some cases. For incoming longwave radiation, even clear-sky estimates show a large degree of scatter, and results degrade substantially if cloudy periods are included. NARP shows improvement over the regression approach. If observations of downwelling longwave radiation are included, NARP and the more complex canopy scheme show similar results, near or within the range of instrument error, depending of time of year.

1. Introduction

Net all-wave radiation ($Q*$) is a fundamental component of surface–atmosphere energy exchange; indeed, it almost always provides most of the energy that drives evaporation and sensible heat fluxes. Despite its importance to these processes, it is rarely observed. Although ostensibly an input to parameterizations of surface layer fluxes, it is more commonly computed from other measured and modeled components of the radiation balance. At the surface $Q*$ can be calculated from incoming shortwave and longwave components provided by an atmospheric radiative transfer scheme as part of a large-scale atmospheric model (Niemelä et al. 2001a,b). Alternatively, without resorting to such numerically intensive methods or requiring vertical profiles of atmospheric properties (for the radiative transfer scheme), $Q*$ may be modeled simply based on near-surface observations of these fields. Representing the radiation exchange within the urban canopy volume of the surface layer presents a greater challenge because of the vertical structure and the range of materials present.

Cities have complex surfaces with a wide variety of materials covering a range of albedo, emissivity, and thermal inertia values. The convoluted nature of the urban surface affects radiation exchange by causing multiple reflections of shortwave radiation and interelement emissions and reflection of longwave radiation, and the increased surface area in comparison with a horizontal plane aids storage of sensible and latent heat. Urban canyons are, therefore, more effective in capturing energy than horizontal surfaces made of the same materials. Modeling these effects has been accomplished by employing a generalized canyon to represent the whole city (averaged characteristics over the urban domain, e.g., urban tile of a grid cell in a mesoscale model) or a distinct urban surface area (at the local or neighborhood scale) (Arnfield 1982; Masson 2000). One difficulty in objectively evaluating such models is how to determine the appropriate surface characteristics of such an inherently inhomogeneous environment. Depending on the model requirements, extensive data collection and/or some adjustment of surface characteristics may be needed to ensure that the model yields results that converge with reality. Though representation of this vertical structure is necessary if the target of interest lies within the urban canyon, above a certain height we may assume that bulk surface characteristics can be applied with nearly the same accuracy. These bulk or effective values define the aggregate response of the conglomeration of materials and geometry over

---

Corresponding author address: Brian Offerle, Atmospheric Science Program, Department of Geography, Indiana University, 120 Student Building, 701 E. Kirkwood Ave., Bloomington, IN 47405-7100.
E-mail: bofferle@indiana.edu

the scale, grid, or tile in question. This approach assumes that the response of individual materials or surfaces (e.g., walls) is not of interest. It also defines the "surface" as the top of a hypothetical volume at a level usually less than 4 times the mean element height or interelement spacing (see Grimmond and Oke 2002). This definition is consistent with surface layer fluxes at this reference height, which should be distinguished from the true surface flux, although in practice the area-averaged fluxes may not be significantly different.

In the present application, we define the scale of analysis to be the local scale (10^2–10^4 m), such that effective characteristics of the type discussed above are applicable. To ensure that observations are consistent with the model scale, we need to consider the field of view of the measuring instrument for the effective surface of interest. Schmid et al. (1991) give the source-area fraction (view factor) P of an inverted flat-plate radiometer as

$$P = 1/(1 + z_m^2/r^2), \qquad (1)$$

where r is the radius defining the source-area fraction and z_m is the measurement height. We can specify (1) in terms of identifiable units, for example, buildings or urban canyons with mean height (H) and spacing or width (W) (Fig. 1a) in order to determine whether the view factor of the instrument adequately captures the effects of multiple buildings. The fraction of net radiation received from an area of N_b building units, $P(N_b)$, assuming they are square with their width equal to the spacing (i.e., assuming in Fig. 1a, $W_x = W_y = L_x = L_y$), is given by replacing r^2 in (1) by $N_b \, 4W^2/\pi$, and substituting $z_m/H \times H$ for z_m:

$$P(N_b) = 1/[1 + \pi(z_m/H \times H/W)^2/(4N_b)]. \qquad (2)$$

This is only an approximation because it does not incorporate radiation from within the canopy or the effects of variation in building heights or arrangement.

Figure 1b shows the relation (2) for a range of aspect ratios in terms of nondimensional height (z_m/H) at level H with $N_b = 2$. With low aspect ratios (e.g., single-family residential areas), a higher measurement height is required relative to H to incorporate the effects of the same number of building units. However, in these cases building heights are typically lower, and so the absolute height required may not be great. For more closely spaced buildings, the height requirement is relaxed; however, the absolute height could be greater relative to ground level. The height requirement for 50% representation from two building units given $H/W = 1$ is $z_m = 2.75H$. This is greater than the minimum height requirement ($2H$) for eddy covariance (EC) flux measurements to be representative at the local scale in urban areas (Grimmond and Oke 1999; Roth 2000). Figure 1c shows the radiative contribution made by a specific number of buildings for an aspect ratio of 1. For example, to achieve 50% representation from five building units requires $z_m = 3.5H$. Thus, Q^* measurements may have more stringent siting requirements than EC. A mit-
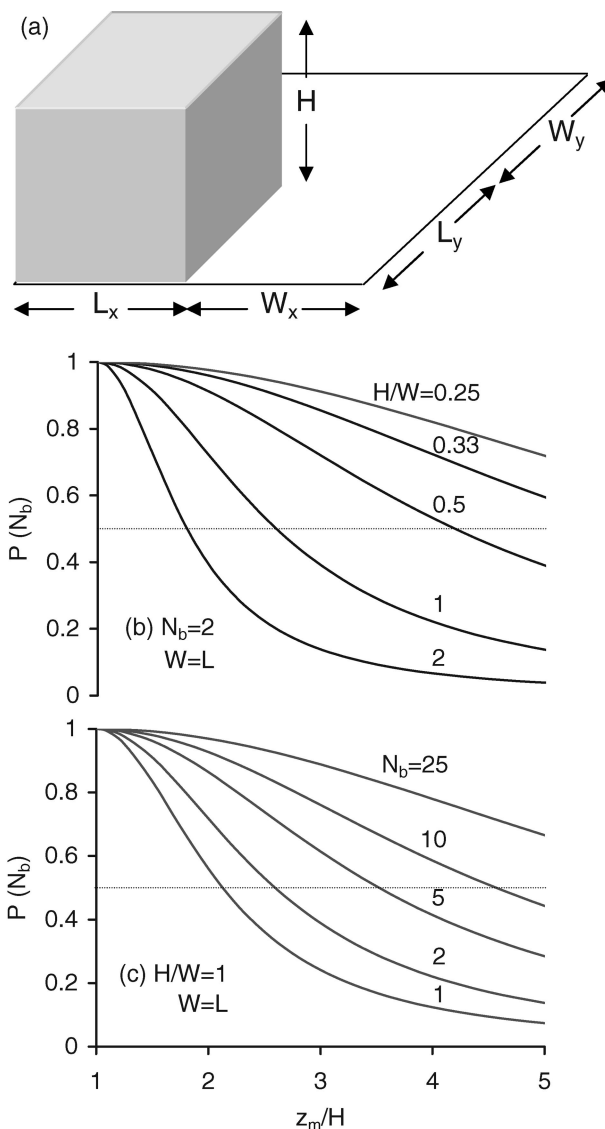
igating factor, however, may be that within the same urban land-cover type, Q^* has been shown to be spatially conservative (Oke 1988; Schmid et al. 1991).

Direct measurements of Q^* are even more uncommon over urban areas than other surfaces. For example, the Atmospheric Radiation Measurement Program (ARM) intentionally excludes urban sites as being "outside of primary interest" (Barr and Sisterson 2000). Consequently, there have been few evaluations of parameterizations over a range of seasonal, climatological, and surface conditions in cities.

Interest here is in the evaluation of a parameterization scheme for Q^* that requires only a minimal set of easily

FIG. 1. (a) Single building–space unit. (b) Source area fraction (P) for upwelling radiation at height H originating from an area of two building units over urban arrays with various aspect ratios (H/W). (c) Same as (b), but for various numbers of building units with fixed $H/W = 1$. See text for definitions.

available measured inputs (meteorological and surface characteristics). This offers the advantage of ease of integration into models that do not include radiative transfer schemes and application to different urban sites, without requiring additional measurements or substantial increases in computation time. Such models have application in predicting surface layer fluxes (Grimmond and Oke 2002) or a meteorological preprocessor for use in the urban boundary layer.

The objectives of this paper are to present the net all-wave radiation parameterization (NARP), which is a modification of earlier work over nonurban surfaces (Holtslag and van Ulden 1983; Crawford and Duchon 1999), and to evaluate NARP using observations from cities with contrasting surface characteristics and climates over the full annual period. The results of NARP are compared with those from a regression model based solely on the availability of incoming solar radiation observations, and from an urban canyon mesoscale surface scheme/tile representation [Town Energy Balance (TEB) Interactions between Soil, Biosphere, and Atmosphere (ISBA)] that uses a more extensive set of inputs. The observations used in the evaluation are from three very different urban sites in Chicago, Illinois; Los Angeles, California; and Łódź, Poland.

2. Parameterization and modeling

a. Regression approach

The radiation budget for a horizontal surface is

$$Q^* = K^* + L^* = K_\downarrow - K_\uparrow + L_\downarrow - L_\uparrow, \quad (3)$$

where K and L represent the short- and longwave components, respectively, the arrows give the direction of the flux, and $*$ is a net flux. Although the preference in developing a simple parameterization scheme of Q^* is to minimize data requirements to only the most commonly available meteorological fields, we find that observations of incoming solar radiation are almost mandatory. While there are many simple relations for $K_\downarrow$, based on latitude and average atmospheric conditions (e.g. Sozzi et al. 1999; Niemelä et al. 2001b), error estimates for hourly intervals or shorter can be large. Niemelä et al. (2001b) used hourly data over 1997 from two sites in Finland. They found root-mean-square errors (rmse) ranging from 12 to 49 W m^{-2} (3.2%–13.7%) for simple models and 11 to 19 W m^{-2} (3.2%–6.0%) for more sophisticated radiation transfer schemes under clear-sky conditions ($N = 26$ and 27 for the two sites). Badescu (1997) examined actinographic data from two sites in Romania during January and July over 10-yr periods. The rmse ranged from 11% to 17% in July ($N = 258$ and 175) and from 15% to 24% in January ($N = 147$ and 94). For all-sky conditions, using total cloud-cover estimates, performance is much poorer with rmse ranging from 30% to 45% (Badescu 1997; Niemelä et al. 2001b). The availability of measured $K_\downarrow$ has the ad-

ditional advantage of allowing estimation of cloud cover and its effects on $L_\downarrow$.

Simple linear regression models of Q^*, based on measured $K_\downarrow$, can generate impressive results, with rmse $<$ 30 W m^{-2} (relative values not reported) (Kaminsky and Dubayah 1997). The general form of such models is

$$Q^* = b_0 + b_1 K_\downarrow, \quad (4)$$

with the b coefficients estimated using ordinary least squares (OLS) regression. Where there is large seasonal variability in terms of external forcing (higher latitudes) and atmospheric effects (transmissivity and emissivity), or surface changes (snow cover, leaf cover, surface moisture), seasonally determined coefficients may improve results (Kaminsky and Dubayah 1997; Iziomon et al. 2000). Implicit inclusion of albedo in (4), by replacing $K_\downarrow$ with K^*, produces mixed results (Kaminsky and Dubayah 1997). Iziomon et al. (2000) found that the inclusion of additional parameters in the regression model had significant effects on model performance only in the case of a mountainous site. Here, the OLS model (4) is compared with NARP.

b. NARP

The model forwarded here is applicable in urban areas where access to other than standard weather observations is limited or zero. To estimate Q^*, the scheme requires air temperature (T_a), relative humidity (RH), and $K_\downarrow$ to estimate Q^*. It is assumed that the measurement height of the instruments corresponds to the reference height for the modeled Q^*. The implication of input bias, due to different instrument placements or larger than normal measurement errors, is addressed with a sensitivity analysis.

1) NET SHORTWAVE RADIATION

The net shortwave term is a function of incoming solar radiation and the bulk surface albedo α_0,

$$K^* = K_\downarrow(1 - \alpha_0), \quad (5)$$

with no distinction made between direct and diffuse radiation. Measured values of α_0 for urban areas typically range from 0.10 to 0.27, with a mean near 0.15 (Oke 1987); $K_\downarrow$ is likely to dominate the daytime radiation budget (Q^*) during summertime, at low latitudes, and if there is no significant cloud cover.

The albedo of a surface varies in response to solar angle and changes in surface characteristics; α_0 generally increases with increasing zenith angle over horizontally homogeneous surfaces (Paltridge and Platt 1976). While other empirical relations have been used (De Rooy and Holtslag 1999; Iziomon et al. 2000), the form

$$\alpha_0(\psi) = \alpha + (1 - \alpha) \exp[-0.1\psi - (1 - \alpha)/2], \quad (6)$$

where α is the albedo at maximum solar elevation and

ψ is elevation angle in degrees (USEPA 1999), is explored in section 4b. In cities, because of the vertical structure and spatial differences in material properties within the source area of the model or measurement domain, this diurnal effect is not just a simple function of solar angle. Sailor and Fan (2002), using a numerical simulation, found that using typical albedo values estimated at nadir, rather than a diurnally varying effective albedo, caused an underestimate of the daily absorbed energy. The decrease was as large as 19% averaged over residential areas, although this value depends on assumptions about the albedos of the roof, wall, and road surfaces. When observing urban albedo, the radiation received by the sensor from the surface may emanate from a different mix of materials, each with different shading by buildings and trees, through the course of a day. Thus, the albedo may exhibit anisotropy with respect to solar angle.

In addition to solar angles and localized changes in shading, albedo can be affected by seasonal changes in surface cover, such as with extensive deciduous vegetation, or due to the effects of snow cover or rain wetting. Brest (1987) found the magnitude of seasonal changes in urban albedo to be inversely correlated with the density of buildings. Although vegetation amounts were not given, presumably the correlation is positive. The impact of snow cover and rain is limited in cities by the vertical surfaces, the albedos of which do not change substantially (Arnfield 1982; Brest 1987). The implications of time-varying albedos can be evaluated by comparing the response using constant albedo with that using a more correctly specified daily albedo ($\alpha_{0,d}$), computed from the direct measurements ($\alpha_{0,d} = K_\uparrow/K_\downarrow$), or that obtained as the residual of the radiation balance (3) (Sozzi et al. 1999),

$$\alpha_{0,d} = (K_\downarrow + L_\downarrow - L_\uparrow - Q^*)/K_\downarrow, \qquad (7)$$

where Q^* and $K_\downarrow$ are observed quantities and the long-wave components are estimated.

2) INCOMING LONGWAVE

One could make an argument similar to that presented for $K_\downarrow$ to include measurements of $L_\downarrow$ in a parameterization for Q^*, because the variability of cloud cover makes estimation of $L_\downarrow$ difficult. Even under clear-sky conditions, estimates of $L_\downarrow$ for cities may be different from measurements because of variability in atmospheric aerosols. When comparing six emissivity formulations for all-sky conditions, Crawford and Duchon (1999, hereinafter CD99) found unsystematic rmse ranging from 10 to 22 W m^{-2} over 4-month periods at nonurban sites. For clear-sky conditions over a wider range of sites, Prata (1996) also compared six formulations (four the same as in CD99) and found rmse of 10–20 W m^{-2}. Because $L_\downarrow$ is less commonly observed than $K_\downarrow$, in the absence of output from a radiative transfer scheme, surface estimation is needed.

To keep the parameterization simple, a single-layer atmosphere model can be used, such that

$$L_\downarrow = \varepsilon_{\text{sky}} \sigma T_{\text{sky}}^4, \qquad (8)$$

where T_{sky} is the bulk atmospheric temperature (K) approximated by T_a near the surface, σ is Stefan's constant, and ε_{sky} is an estimated broadband atmospheric emissivity. Surface-level schemes for clear-sky emissivity ($\varepsilon_{\text{clear}}$) have been reviewed in detail elsewhere (Sugita and Brutsaert 1993; Prata 1996; CD99; Niemelä et al. 2001a). The Prata (1996) formulation,

$$\varepsilon_{\text{clear}} = 1 - (1 + w) \exp[-(1.2 + 3.0w)^{0.5}], \qquad (9)$$

has been found to perform best (Prata 1996; Niemelä et al. 2001a), including tests at an urban site (Newton 1999). In (9), w is the precipitable water content (g cm^{-2}) approximated by mean atmospheric values of vapor pressure (e_a) and T_a at the reference height in the surface layer:

$$w = 46.5 \, e_a/T_a.$$

Cloud effects on $L_\downarrow$ are harder to generalize because rather than just cloud fraction, both cloud height (especially cloud-base temperature) and type have radiative impacts. In general, ε_{sky} should increase toward unity as total cloud cover, depth, and cloud-base temperatures increase. The ratio of measured $K_\downarrow$ to that predicted under clear-sky conditions ($K_{\downarrow,\text{clear}}$) can give an objective estimate of daytime cloud effects related to cover amount and depth; $K_{\downarrow,\text{clear}}$ is estimated by (CD99)

$$K_{\downarrow,\text{clear}} = I_{\text{Ex}} \cos(Z)\tau_R \tau_{\text{pg}} \tau_w \tau_{\text{aer}}, \qquad (10)$$

where I_{Ex} is extraterrestrial solar insolation, Z is the solar zenith angle, and $\tau_R \tau_{\text{pg}} \tau_w \tau_{\text{aer}}$ is the product of transmissivities for Rayleigh scattering (R), absorption by permanent gases (pg) and water vapor (w), and absorption and scattering by aerosols (aer). The transmissivities are a function of time of year, zenith angle, latitude, surface dewpoint (computed from T_a and RH), and surface pressure. Although incorporating an observation of local pressure adds an additional input requirement, this measurement is routinely available and varies gradually spatially, such that values from the nearest station after correction for elevation can be used. The Smith (1966) data used in the formulation of CD99 were interpolated to an array of 1° latitude for each day of the year to facilitate application to the model developed here.

The daytime cloud fraction (F_{CLD}) is then given by (CD99)

$$F_{\text{CLD}} = 1 - K_\downarrow/K_{\downarrow,\text{clear}}. \qquad (11)$$

This method of determining F_{CLD} becomes unreliable at large zenith angles because of the cosine response of pyranometers, and especially to the small magnitude of $K_\downarrow$. A similar situation is encountered using the clearness index (CI = $K_\downarrow/I_{\text{ex}}$); hence, Sugita and Brutsaert (1993) limited their analysis to observations where $K_\downarrow > 30$ W m^{-2}. Battles et al. (2000) also found that clear-sky solar

irradiance parameterizations performed less well at high zenith angles. Here, we take note of these errors by limiting transmissivity computations to zenith angles $<80°$. This results in an overestimate of cloud cover at higher zenith angles, which, in turn, biases estimates of $L_\downarrow$ at these times. This is an issue at night when no cloud estimate with (11) is possible and the choice is either no adjustment or basing the cloud estimate on the sunset value, which may well be biased. Here, the latter is preferred as long as the error remains small.

Clear-sky emissivity is then adjusted for the effects of cloud cover:

$$\varepsilon_{sky} = \varepsilon_{clear} + (1 - \varepsilon_{clear})F_{CLD}^2. \quad (12)$$

The squared term is intended to minimize the effect of the biased cloud cover while still allowing for $\varepsilon_{sky} = 1$. The performance of this, or other parameterizations of longwave cloud effects, depends on site cloud climatology. The above approach does not account for the effects of cloud type (height of cloud base) on emission. Sugita and Brutsaert (1993) find that including cloud type improves the emissivity estimation, because lower clouds have a much greater impact. It may be useful to incorporate this, but for the purposes of the present study the additional input requirement was deemed undesirable.

3) OUTGOING LONGWAVE

Outgoing longwave radiation from the surface,

$$L_\uparrow = \varepsilon_0 \sigma T_0^4 + (1 - \varepsilon_0)L_\downarrow, \quad (13)$$

is primarily driven by the effective radiative surface temperature T_0; only a small fraction is due to the reflection of $L_\downarrow$ from the surface (the second term). For a large area, T_0 is difficult to determine directly, and it is almost never available from routine observations. This makes it necessary to substitute an approximation of T_0 by near-surface T_a in (13). However, this tends to introduce a systematic diurnal bias because surface temperatures are greater (less) than near-surface air temperatures by day (night). The estimate is particularly biased during the daytime. Traditionally (Sellers 1965; Holtslag and van Ulden 1983), this bias is corrected by using

$$\varepsilon_0 \sigma T_0^4 \approx \varepsilon_0 \sigma T_a^4 + 4\varepsilon_0 \sigma T_a^3(T_0 - T_a). \quad (14)$$

For the daytime case, the last term can be based on either Q^* or $K_\downarrow$. Here, we use $K_\downarrow$ to develop a correction, because $K_\downarrow$ is an observed quantity in the parameterization. The magnitude of this correction is estimated by

$$4\varepsilon_0 \sigma T_a^3(T_0 - T_a) = cK_\downarrow(1 - \alpha_0), \quad (15)$$

which is a modification of the form given by Holtslag and van Ulden (1983) that did not incorporate α_0. Note that van Ulden and Holtslag (1985) revised their original formulation to incorporate α_0 and the slope of the saturation enthalpy curve but used Q^*. As formulated here,

with $\alpha_0 = 0.15$, $K_\downarrow = 1000$ W m^{-2}, $T_a = 300$ K, and using $c = 0.08$ [approximated from Holtslag and van Ulden (1983)], the correction is equivalent to $T_0 - T_a = 11$ K. This seems appropriate for a dry surface. However, this approach does not account for any hysteresis in $T_0 - T_a$, and at night it results in no correction at all. In practice, T_0 should peak after $K_\downarrow$, approach T_a near sunset, and may become cooler than T_a at night under stable conditions. However, these differences are likely to be small relative to the overall correction. Further, the lack of a nocturnal correction may be more acceptable in urban areas, especially city centers. This is because the nocturnal release of stored heat from the urban fabric is substantial, sufficient enough to produce upward-directed convective sensible heat fluxes (Grimmond and Oke 2002) and temperature profiles that tend toward neutral (Oke 1995). The lack of a nighttime $T_0 - T_a$ correction is likely to have little impact relative to the errors associated with cloud cover and ε_{sky} determinations. However, by integrating this parameterization with a surface heat-flux model, stability could be calculated and a better estimate of T_0 might be made (van Ulden and Holtslag 1985; De Rooy and Holtslag 1999). Also in question is the time constant of the effective surface temperature, which determines the most appropriate averaging interval over which to implement this correction. To minimize the impact of short-term variations in $K_\downarrow$ due to clouds, the correction is implemented using values from the previous hourly average. The complete $L_\uparrow$ specification can be written:

$$L_\uparrow = \varepsilon_0 \sigma T_a^4 + 0.08K_\downarrow(1 - \alpha_0) + (1 - \varepsilon_0)L_\downarrow. \quad (16)$$

The complete parameterization scheme is specified by Eq. (5) for the shortwave balances, Eqs. (8)–(12) for incoming longwave, and Eq. (16) for outgoing longwave.

4) RADIATION SCHEME OF THE TEB ISBA MODEL

The radiation scheme from the TEB urban canopy-layer parameterization of Masson (2000), coupled with the ISBA model (Noilhan and Planton 1989) is also used to evaluate the effectiveness of NARP. Since the original publication of TEB there have been several modifications to the code and the latest version was used for this evaluation (V. Masson 2003, personal communication). TEB divides the urban canopy into three distinct surfaces: roofs, walls, and roads. Radiative characteristics (α, ε) must be specified for all surfaces, as well as the thermal characteristics of multiple layers within the roofs, walls, and roads to allow for heat diffusion and computation of the surface temperature. Within the urban canyon, constant view factor geometry and no preferred orientation of the streets are used to determine the radiation balance for the walls and roads. Surface temperatures are calculated from thermal characteristics and the energy balance at each time step. Given the input demands of TEB ISBA in terms of surface char-

acteristics, and because it requires $L_\downarrow$ observations as input, this model was only run for one site (Łódź).

3. Site and measurement characteristics

a. Instrumentation

NARP is evaluated using observations from three sites: Chicago (1992–93), Los Angeles (LA) (1993–94), and Łódź (2001) (Table 1). These research sites were established to make energy balance flux observations and were situated in areas suitable for eddy covariance flux measurements (Grimmond and Oke 1999; Roth 2000). While these observations were not designed primarily as radiation studies, they happen to represent three very different urban surface systems. Hence, if a scheme performs well using these datasets, it is likely to indicate more general applicability. In Chicago and Los Angeles, Radiation and Energy Balance Systems (REBS) $Q*6$ net radiometers measured $Q*$, and LI-COR pyranometers (LI-200) monitored $K_\downarrow$. In Łódź, a Kipp and Zonen CNR1 measured the four component fluxes of the radiation budget. No snow-cover observations were made at either the Chicago or Łódź sites. In Chicago and Los Angeles, the T_a and RH sensors were housed in aspirated shields, whereas in Łódź an unaspirated Gill shield was used. In all cases the T_a and RH sensors were located close to the net radiometers. The measurement height was at least 2 times the mean canopy height for all sites (Table 1). All data were recorded as 15-min averages. Greater details about site characteristics and operational information may be found in Grimmond et al. (1994, 1996) and Offerle et al. (2002).

The accuracy of the $Q*6$ sensor is subject to some debate. Hodges and Smith (1997) report that the $Q*6$ underestimates nighttime flux densities by approximately 45% (when compared with individually calibrated Eppley pyrgeometers). They also reported daytime underestimation of 5%. Duchon and Wilk (1994) also note similar nighttime discrepancies. The manufacturer examined this issue in controlled field and chamber tests and reached a different conclusion (C. Fritschen 2002, personal communication). Because of the lack of agreement between published results and the manufacturer's recommendation, we applied no correction. Assuming this results in a systematic bias, the effect should be similar in both Chicago and Los Angeles. The results of Hodges and Smith (1997) suggest that this bias will be negative when compared with the CNR1. The LI-200 sensor used for $K_\downarrow$ has an absolute error of 5% (LI-COR 1991).

The expected CNR1 accuracy for daily totals of $Q*$ is $\pm10\%$ (Kipp and Zonen 2001). Oncley et al. (2002) found that the CNR1 performed well for $Q*$, although individual component fluxes were more in error. Longwave measurements are known to be affected by dome or window heating, particularly at times of low wind speed. In the CNR1, the body temperature of the in-

TABLE 1. Site information, model parameters, and dataset characteristics. Mean $Q*$ values are for all-sky conditions restricted to time periods available at all sites; N_b was identified using aerial photographs.

Site	Latitude, longitude	Observation period (year/day of year)	Instrument	z_m (m)	z_m/H	N_b (90%)	α_0	ε_0	Clear-sky days	Mean $Q*$ (W m^{-2}) Day	Mean $Q*$ (W m^{-2}) Night
Chicago	41°57'N; 87°48'W	1992/198–1993/158	$Q*6$	25	3.0	3	0.18	0.93	25	158	−31
Los Angeles (A94)	34°08'N; 118°03'W	1993/225–1994/206	$Q*6$	30	2.8	14	0.21	0.94	79	255	−48
Łódź	51°46'N; 19°27'E	2001/001–365	CNR1	37	2.2	14	0.08	0.92	20	137	−38

strument is used to correct for this effect. To avoid condensation on the domes and windows (receiving plates) of the CNR1, the instrument was heated, but only at night. Heating typically affects shortwave more strongly than longwave readings; hence, restricting it to the night should reduce the potential for errors (Kipp and Zonen 2001). The radiometer domes of the sensors in Chicago and Los Angeles were not heated and, thus, may have been affected by condensation. The radiation instruments were calibrated by the manufacturers prior to use in these measurement campaigns. Although all data were subjected to strict data limits to prevent unreasonable values, these errors would be biased toward zero and, as such, were probably not detected. With the exception of known periods of instrument malfunction, no other data were rejected. Clear-sky days were identified by visual inspection of the curves for incoming solar radiation (numbers noted in Table 1). Los Angeles routinely experiences early morning low-level cloud cover that typically dissipates by late morning. This has been observed at the study site (Grimmond et al. 1996). Because of this early morning cloudiness, the Los Angeles clear-sky data are restricted to times later than 1100 (local time).

The daily mean Q^* over the datasets for the three sites is shown in Fig. 2. All sites exhibit day-to-day variability throughout the year because of changes in the local cloud cover. Because of the incomplete data for Chicago and Los Angeles (LA), only the time periods when data are available for all sites are used for the means reported in Table 1. This aids comparison; however, these are not true annual means.

b. Estimated parameters

Measured values for albedo and emissivity are not available for most urban locations. To evaluate the effect of using general tabulated values on model performance, the surface albedo and emissivity for Chicago and LA were estimated using only general site characteristics and values taken from the literature. In Chicago, the instrument tower (approximately 4 km southeast of O'Hare International Airport) is surrounded by short commercial and institutional buildings with mixed vegetation (trees and grass). The LA tower is located in the residential neighborhood of Arcadia with mixed vegetation (trees, shrubs, and bare sandy soil). The Łódź site, located near the urban core, is surrounded by 15–20-m-tall buildings.

For Chicago and LA, the 50% and 50%–90% radiative source-area fractions were determined using (1). The dominant surfaces in Chicago were asphalt paving (36%) and short grass (29%), with roofs making up 16% of the weighted source-area fraction. In Los Angeles, trees (deciduous and evergreen) contributed 33% of the surface cover, with roofs and asphalt paving contributing only 15%. Effective α_0 and ε_0 (Table 1) were calculated from weighted averages of surface-cover
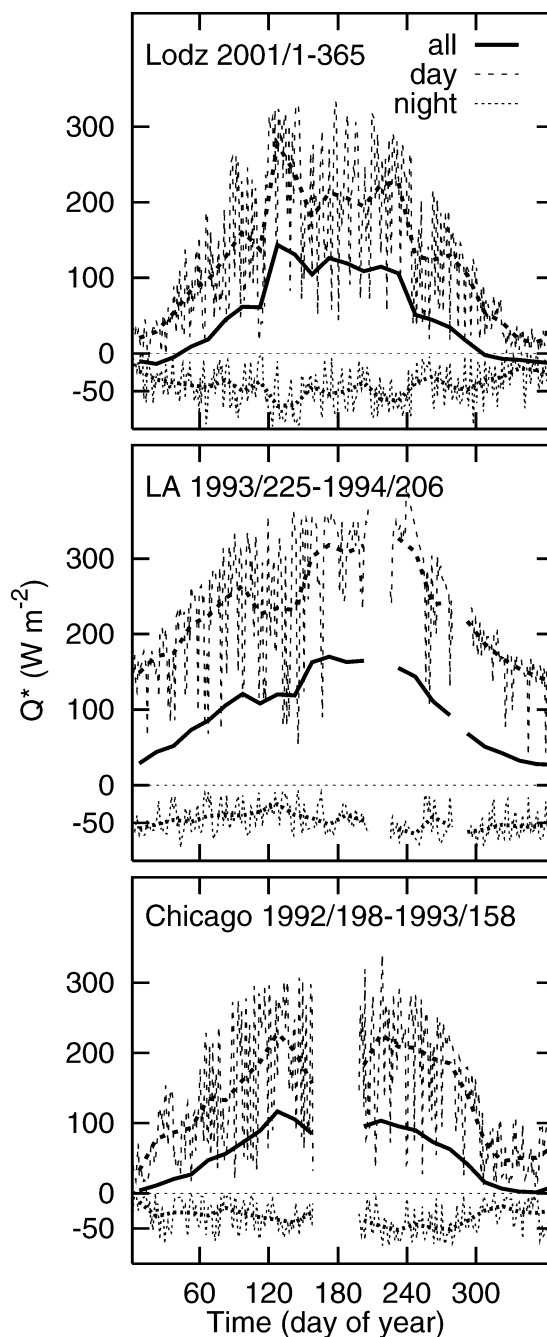

FIG. 2. Daily average Q^* (W m^{-2}) measured at (top) Łódź, (middle) Los Angeles, and (bottom) Chicago, in the daytime ($Q^* > 0$) and at night ($Q^* < 0$). Thicker lines are 15-day block averages. Note periods of missing data for Los Angeles and Chicago.

types, as found in published tables (Arnfield 1982; Oke 1988). Because it was available for Łódź, the annual median measured albedo (0.08) was used, and ε_0 was set equal to the weighted average (0.92) of the TEB input emissivities (Table 2). This value is lower than the 0.94–0.96 calculated by Arnfield (1982).

The TEB ISBA scheme was only evaluated for Łódź,

TABLE 2. Input parameters used in the TEB model calculations for Łódź.

Urban surface	Plan area fraction[a]	α[b]	ε[c]	Layer	Depth (m)	Heat capacity[d] (MJ m^{-3} K^{-1})	Thermal conductivity[d] (W m^{-1} K^{-1})
Roof	0.32	0.06	0.92	1 tar and gravel	0.01	1.95	0.90
(H = 17 m)				2 tar and gravel	0.05	1.95	0.90
(H/W = 1.0)				3 concrete	0.05	1.50	0.93
				4 cement	0.01	1.30	0.37
Wall	—	0.15	0.90	1 cement/windows	0.02	1.45	0.53
				2 brick	0.20	1.60	0.70
				3 brick	0.20	1.60	0.70
				4 cement	0.02	1.30	0.37
Road	0.38	0.11	0.94	1 asphalt/concrete	0.02	1.83	0.79
				2 asphalt/concrete	0.08	1.83	0.79
				3 gravel/sandy clay	0.50	1.40	0.40
				4 gravel/sandy clay	0.50	1.40	0.40

Sources: [a] K. Klysik (2001, personal communication); [b] K. Fortuniak (2002, personal communication); [c] Oke (1987); [d] ASHRAE (1981); Meyn (2000); Masson et al. (2002).

because it requires both fairly detailed surface characteristics and an observed value for $L_\downarrow$ (not directly measured in Chicago and LA). The ISBA portion of the scheme is used for the vegetated fraction, which was 30%, as determined from a surface database. The radiative properties of roofs, walls, and roads were based on measurements made at the site for albedos (K. Fortuniak 2002, personal communication) and tabulated values for emissivities. The effective albedo calculated from the scheme was higher than the observed value (0.09 versus 0.08), so it is expected that the results will be biased. The choice of thermal characteristics for roof, wall, and road layers were compiled from observations made at the site and from published data (Table 2).

4. Results

The three models (OLS, NARP, and TEB ISBA) are evaluated using the observed data. As a basis for model comparison, we use the mean bias error [MBE = $1/N$ $\Sigma(P - O)$] and the rmse { =[(1/N) Σ $(P - O)^2$]$^{1/2}$}.

a. Regression model results

The coefficients b_0 and b_1, of the OLS model (4) relating net all-wave radiation to incoming solar radiation, are given in Table 3. The input data represent 30% of the observed data selected randomly. In Chicago and Łódź, only snow-free observations were used. For Chicago, determination of snow cover was based on gridded data (Climate Prediction Center 1999), and for Łódź snow cover was assumed when surface wetness was present and $T_a < 0°C$.

The slope value (b_1) is an expression of how effective the surface is in converting the radiative exchanges into net (or absorbed) all-wave radiation. Because this efficiency relates not only to both solar and infrared radiation exchanges, but also to those of sensible and latent heat leading to surface temperature change, no simple surface or atmospheric control on the slope is to be anticipated (Idso et al. 1969). However, in general, we might hypothesize that, ceteris paribus, a site with lower albedo, lower emissivity, higher surface moisture availability, higher surface thermal admittance, and greater roughness should result in greater absorption (larger slope). The slope coefficients for the three cities (Table 3) are higher than those for grassland sites, which average around 0.6, and lie within the range of forests (Kaminsky and Dubayah 1997; Iziomon et al. 2000). Łódź, the site with the lowest albedo, lowest emissivity, and probably the highest thermal admittance, has the greatest slope. It is not obvious why the other two sites are ordered the way they are; however, the radiometer source areas for these sites contain considerably more vegetation (grass in Chicago and trees at the LA site with the area receiving frequent irrigation). The R^2 values and standard errors for the urban sites are similar to results over natural vegetation (Kaminsky and Dubayah 1997; Iziomon et al. 2000).

When these coefficients derived from 30% of the data are used to estimate the net all-wave radiation over the remainder of the dataset, rmse range from 25 to 31 W m^{-2} in the daytime and from 22 to 34 W m^{-2} at night (Table 3). The major disadvantage of using the OLS method is that the coefficients are likely to be place specific. In the absence of data for a given city and knowledge of how to select values for b_0 and b_1 objectively, one can presume that Q^* estimates based on an OLS equation will give greater errors than those in Table 3.

b. Evaluation of NARP subcomponents

Several modifications have been made to existing component models in NARP, notably diurnal and daily albedos, clear-sky solar irradiance, and corrections to outgoing longwave radiation. Because these have not been evaluated for urban surfaces, the effect of each

TABLE 3. OLS estimates of Q^* from measured $K_\downarrow$. Model development: statistics derived using 30% of available Q^* and $K_\downarrow$ data selected randomly. Evaluation: performance statistics using the derived OLS model on the remainder of the data. Values for Q^* are mean of observations. Only snow-free data are used, and N is the number of 15-min data points used in the analysis.

| | Model development | | | | | Evaluation | | | | | |
| | | | | | | N | | Q^* (W m⁻²) | | Rmse (W m⁻²) | |
Site	N	b_0 (W m⁻²)	b_1	R^2	Standard error (W m⁻²)	Day	Night	Day	Night	Day	Night
Łódź	10 167	−38.8	0.80	0.96	32.0	11 438	12 409	153	−42	30.8	33.5
Los Angeles	9344	−47.1	0.72	0.98	29.6	10 553	11 114	236	−47	35.3	22.1
Chicago	7324	−31.6	0.67	0.97	25.0	8360	8685	161	−35	25.1	25.0

change is considered prior to evaluation of the complete Q^* scheme.

The diurnal albedo parameterization (6) was reestimated for Łódź, using clear-sky observations ($N = 997$), to yield

$$\alpha_0(\psi) = \alpha + (1 - \alpha) \exp[-0.2\psi - (1 - \alpha)/2]. \quad (17)$$

The coefficient for elevation decreased from that given in (6) (-0.2 versus -0.1), thereby reducing dependence on elevation angle. Figure 3a shows reflected solar radiation flux densities for Łódź, determined with a constant albedo, while Fig. 3b shows results with the diurnal variation of albedo modeled using (17) and observations not used in the derivation. Comparing Figs. 3a and 3b, it is evident that the effect of including the diurnal variation of albedo is relatively small, less than 20 W m⁻² in all cases. Although the observations follow the functional form of the model (Fig. 3c), other factors (e.g., snow cover) limit the overall improvement in rmse to 0.6 W m⁻². For purposes of general application to urban sites, incorporating diurnal variation of albedo is unlikely to significantly improve the model accuracy and, hence, it is not included in the final form of NARP.

For all sites, the varying daily albedo $\alpha_{0,d}$ was calculated (7) by averaging incoming and outgoing solar fluxes over the period from 1000 to 1400 h local time, during predominately cloud-free periods [$F_{CLD} < 0.2$, (11)], creating a single value for each day. This time period was selected so that the error in modeled L^* is small relative to Q^*. The availability of measured albedo in Łódź allows the estimate, using (7), to be evaluated (Fig. 4). Linear regression analysis of results for 179 days gives a fit with $R^2 = 0.77$, a slope of 0.96, an intercept of 0.02, and an rmse of 0.025 or 26% of the mean observed value. Although the relative error is large, the correlation between the observed and modeled $\alpha_{0,d}$ for Łódź demonstrates that the method is not overly sensitive to errors in estimation of L^*. When averaged over longer periods (the lines on Fig. 4 are 10-day block averages) the performance improves ($R^2 = 0.90$, rmse $= 0.019$). Because we are interested in estimating longer-term variations in albedo, a 15-day moving average $\alpha_{0,d}$ is used in subsequent analyses.

Figure 4 also shows a weak seasonality in albedo in Łódź and that there are differences among the three sites. The albedo in Łódź, which is characterized by a higher density of buildings and greater amount of vertical surface area than the other two sites, exhibits little change from day 90 to day 270, with the 10-day average ranging from 0.09 to 0.07. The 10-day average albedo at the Los Angeles site ranges from 0.20 to 0.13, and at the Chicago site ranges from 0.23 to 0.16. The large peaks in Fig. 4 for Chicago and Łódź are due to snow cover. Even with snow cover, the albedo remains generally lower in Łódź (0.20–0.35) than in Chicago (0.25–0.45). This may be due to the fact that in Chicago, buildings are shorter and more widely spaced. This agrees with the trend in results computed by Arnfield (1982), but is
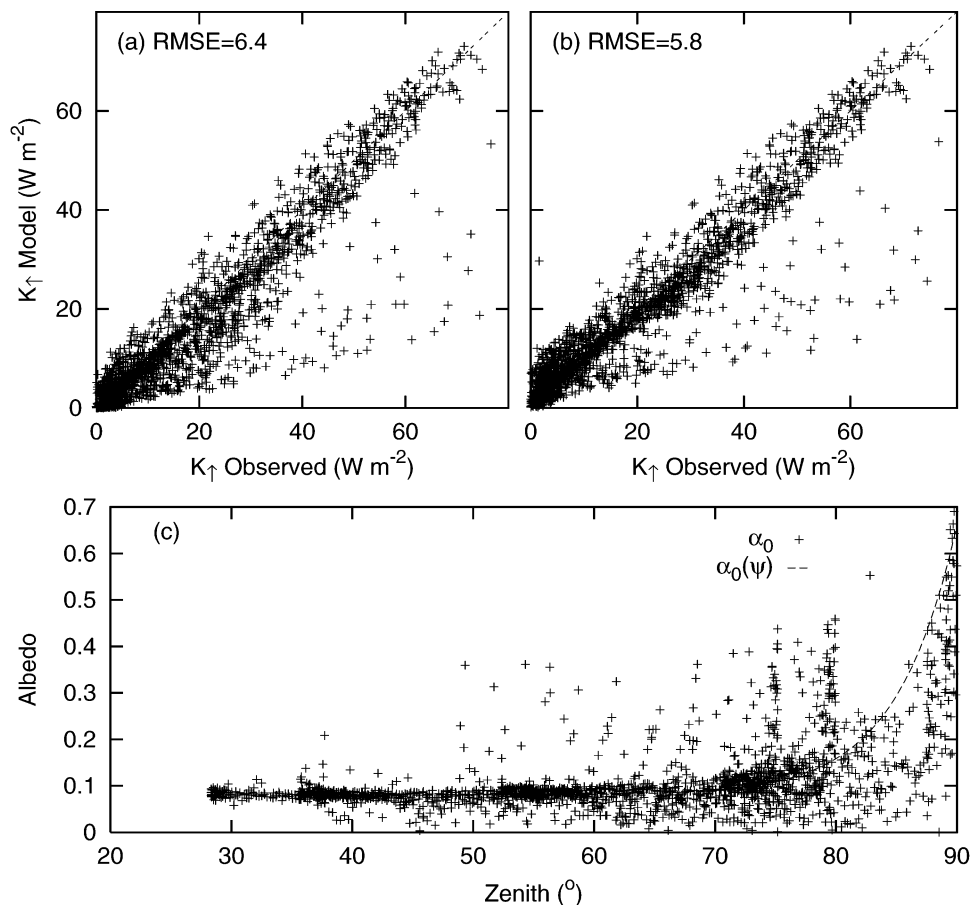
FIG. 3. (a) Comparison of modeled vs observed $K_\downarrow$ for Łódź, using a constant albedo (α_0). Dashed line denotes one-to-one correspondence. (b) Same as (a), but using modeled diurnal albedo [$\alpha_0(\psi)$] that includes diurnal variation calculated from (17). (c) Measured and modeled albedo [$\alpha_0(\psi)$] plotted with respect to solar zenith angle. Data shown were not used in model estimation.

not conclusive because sensor bias would affect the results. Excluding snow cover, the curves do not seem to follow those developed by Brest (1987), who calculated slightly lower wintertime albedos from Landsat imagery for New York. Arnfield (1982) suggests that the low solar elevations in winter in high-latitude cities allow less direct solar radiation to penetrate canyons. The reduced trapping results in higher wintertime albedos.

The annual median albedos estimated from (7) were 0.08, 0.17, and 0.21 for Łódź, Los Angeles, and Chicago, respectively. These values agree with those modeled by Arnfield (1982) for commercial and residential areas similar to the real-world sites used here. The median albedos for Los Angeles and Chicago differ from those determined by surface cover analysis (Table 1) by +0.04 and −0.03, respectively.

The calculated cloud fraction (Fig. 5) shows a strong dependence on zenith angle. This results in an overestimation of $L_\downarrow$ at high zenith angles (Fig. 5). Despite the nonzero values for F_{CLD} at all zenith angles, the effect on $L_\downarrow$ is relatively small because F_{CLD} is a squared term in the adjusted emissivity formulation (12). Until

the zenith angle reaches approximately 75° the $L_\downarrow$ error is within 5%. In part this may be due to increased sensor error at higher zenith angles, but, more probably, it is a limitation of the method used to estimate $K_{\downarrow,clear}$. Because $L_\downarrow$ is actually underestimated at lower zenith angles, it could be argued that cloud effects on emissivity should be increased. However, until the problem at high zenith angles is corrected, this would lead to large errors at sunrise, sunset, and nighttime.

Unfortunately, limitations in accurately estimating $L_\downarrow$ are not restricted to high zenith angles. Figure 6 shows modeled versus observed $L_\downarrow$ for (a) clear-sky days (daytime only), (b) all-sky data, both using ε_{clear}, and (c) all data using the cloud-corrected emissivity [ε_{sky}, Eq. (12)]. In (a), results using the Prata ε_{clear} formulation agree fairly well with observations on occasions when clear skies are visually identified. For this case there is little bias, which is consistent with earlier results (Prata 1996; Newton 1999). On the other hand, in (b), under cloudy skies with no correction, the distribution is bimodal. The group on the one-to-one line represents occasions with high or no clouds; hence, incoming long-
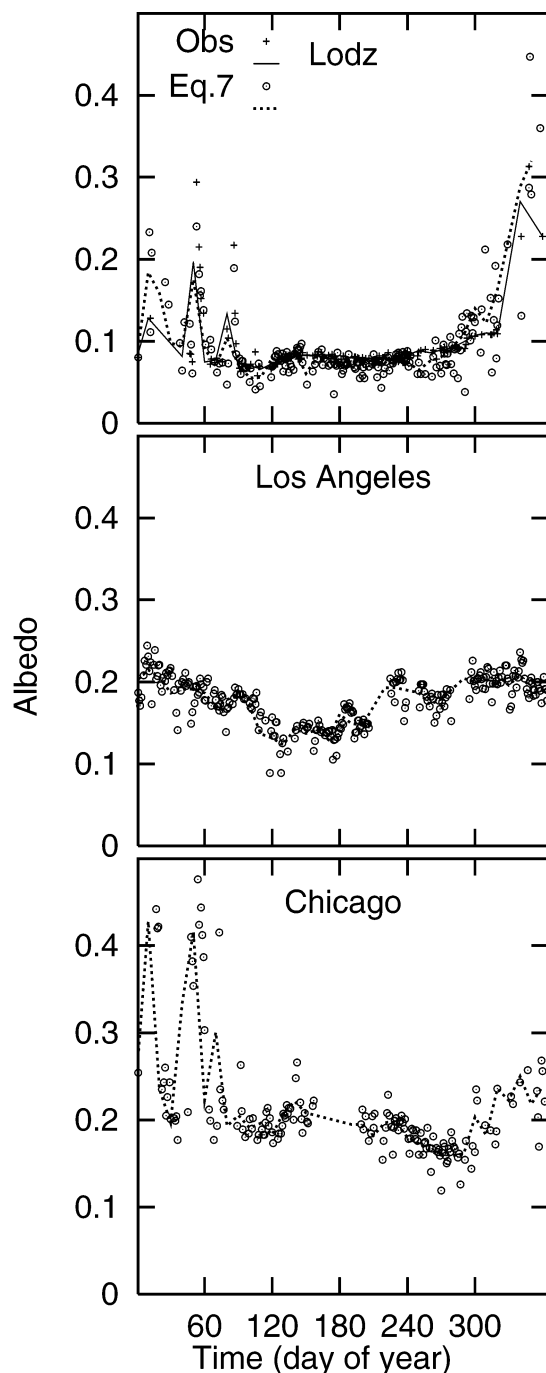
FIG. 4. Daily albedo ($\alpha_{0,d}$) for (top) Łódź, (middle) Los Angeles, and (bottom) Chicago. Directly measured values for Łódź (obs), and those calculated from Eq. (7) for all sites. Lines represent 10-day block averages.
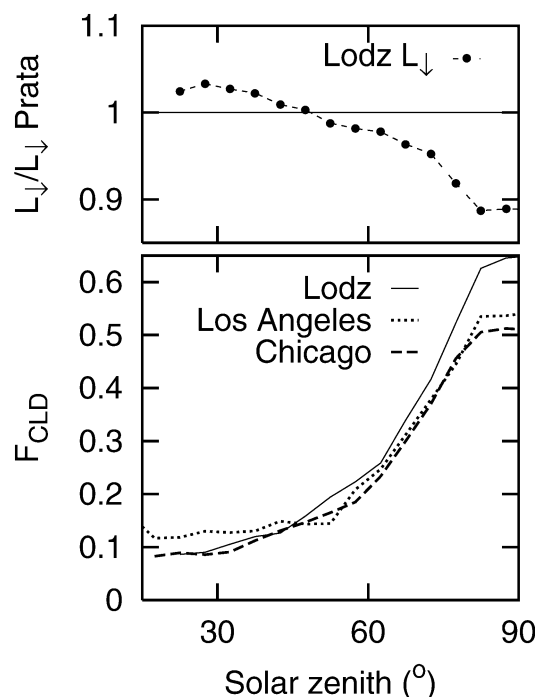

FIG. 5. (bottom) Model average F_{CLD} estimates for clear-sky days vs solar zenith angle. As the zenith angle increases, F_{CLD} increases as an artifact of the model. (top) The impact on modeled sky emissivity causes the modeled $L_{\downarrow Prata}$ to exceed the observed value at large zenith angles (shown for Łódź only).

is not restricted to nighttime, but is often greater at that time because of the limitations in estimating nighttime cloudiness.

Simply replacing T_0 with T_a in the formulation for $L_\uparrow$ leads to large bias errors during the daytime at these urban sites (Fig. 7a). Although the simplified correction (13)–(14) has the shortcomings noted in section 2b(3), the daytime errors are greatly reduced (Fig. 7b). Under clear-sky conditions, when errors attributable to ($T_0 - T_a$) may be expected to be greatest, peak values are still somewhat underestimated but nighttime errors are typically small (Fig. 7c). The correction also captures short-term changes in effective surface temperature even though air temperatures vary little (e.g., see days 186 and 187; Fig. 7c). Nighttime errors are larger when inversions are present as might be the case on the night 190, following a cloudy day.

c. Evaluation of NARP

To test the performance of NARP, two cases were examined for each site:

- case 1, using the specified parameter values from Table 1; and
- case 2, replacing α_0 with the 15-day moving average of $\alpha_{0,d}$.

Analysis is divided into daytime ($K_\downarrow > 5$ W m^{-2})

wave radiation is unaffected. The second group is offset by approximately 75 W m^{-2}, suggesting consistent cloud climatology. In (c), with the cloud correction, the bimodality is removed and the result is largely unbiased (MBE = 3.5 W m^{-2}), but considerable scatter remains. As can be seen in the time series plot (Fig. 6d) this error
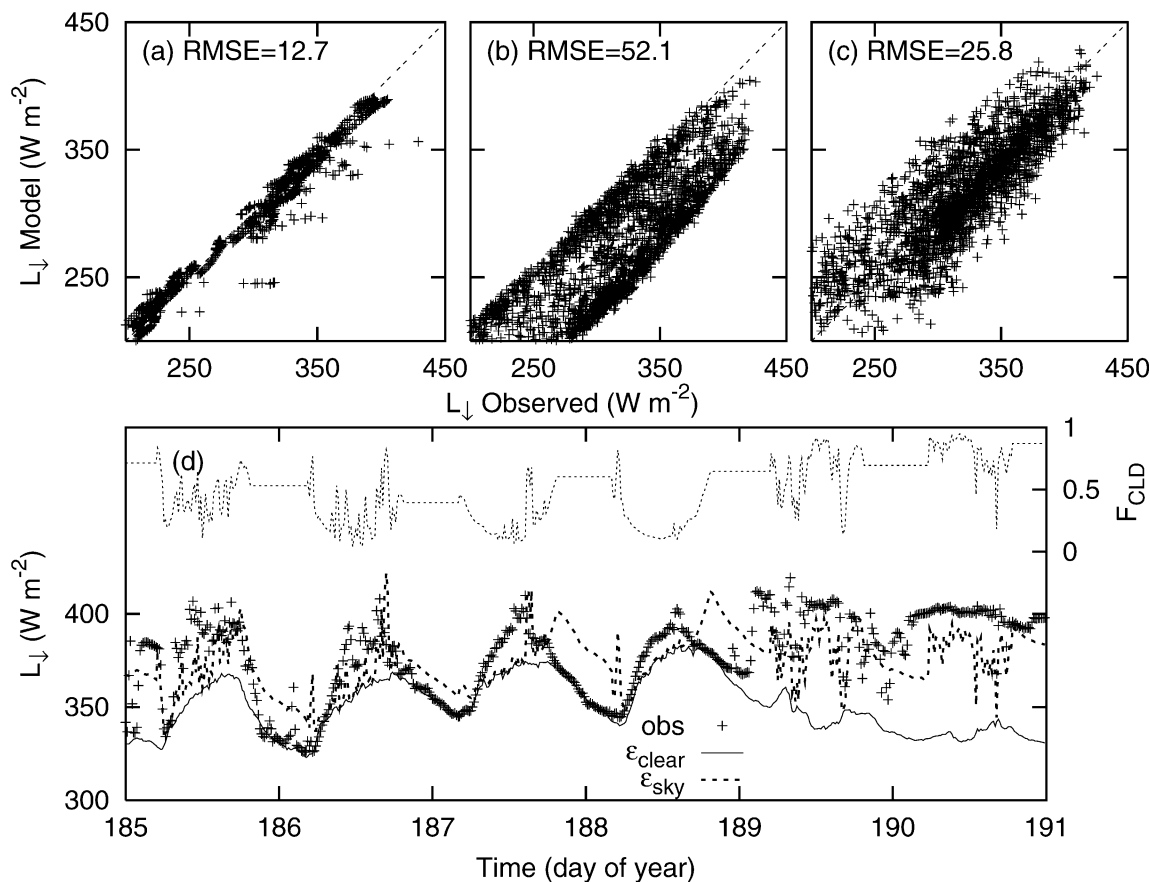
FIG. 6. Modeled vs observed $L_\downarrow$ for Łódź. (a) Visually identified clear-sky days. (b) All observations with no emissivity correction. (c) Same as in (b), but emissivity corrected for cloud cover using (12). (d) Partial time series of estimated cloud fraction and $L_\downarrow$ (including observed, calculated using no emissivity correction for clouds, and using cloud corrected). For clarity in (b) and (c) not all points are shown.

versus nighttime, and "summer" ($121 <$ day of year < 244) (when $K_\downarrow$ is relatively larger) versus "winter" cases. This criterion for day–night separation was selected in lieu of zenith angle or $Q*$ because $K_\downarrow$ is an observed quantity, and also because it reduces the chance of positive sensor offset causing miscategorization. The distinction between summer and winter does not correspond to the true seasonality at the sites but was fixed at dates ensuring no snow cover occurred in the summer period.

1) DAYTIME RESULTS

The base case specification for all sites shows improvement over the OLS model (Tables 3 and 4). The only exception is the case of Los Angeles in summer. It can be seen from Fig. 4 that this is due to having misspecified the albedo for this period. For Chicago and Łódź, daytime values have low bias errors ($|$MBE$| <$ 5% of $Q*$), indicating that the albedo estimated for Chicago was appropriate for an annual mean, and that the model is essentially unbiased for the measured albedo in Łódź. Using the daily computed values for albedo

(case 2) leads to improvement at all sites and times (Table 4), particularly for Los Angeles, but also for Chicago because this accounts for the albedo of snow cover better than the estimates of snow cover and the fixed albedo. Use of the daily computed value for Łódź changes results little. This is to be expected because the albedo of Łódź is low and nearly constant throughout the year (Fig. 4), resulting in only small changes in reflected shortwave radiation.

The bias errors for case 2 are all negative, and in some cases more so than for case 1. If we attribute this to the longwave portion of the model, either $L_\uparrow$ is overestimated or $L_\downarrow$ is underestimated. The first is unlikely because $L_\uparrow$ is seen to be underestimated for Łódź, while $L_\downarrow$ is also underestimated (section 5b and Figs. 5 and 7). The choice of function in the cloud model is the probable cause of this bias. In all cases the bias error is within the presumed range of instrument error.

The daytime results are characterized by small bias errors and relatively little scatter. As can be seen in the results for case 2 (Fig. 8), there few obvious differences in model fit. Figure 9 shows histograms of errors (predicted − observed) for both NARP and the OLS
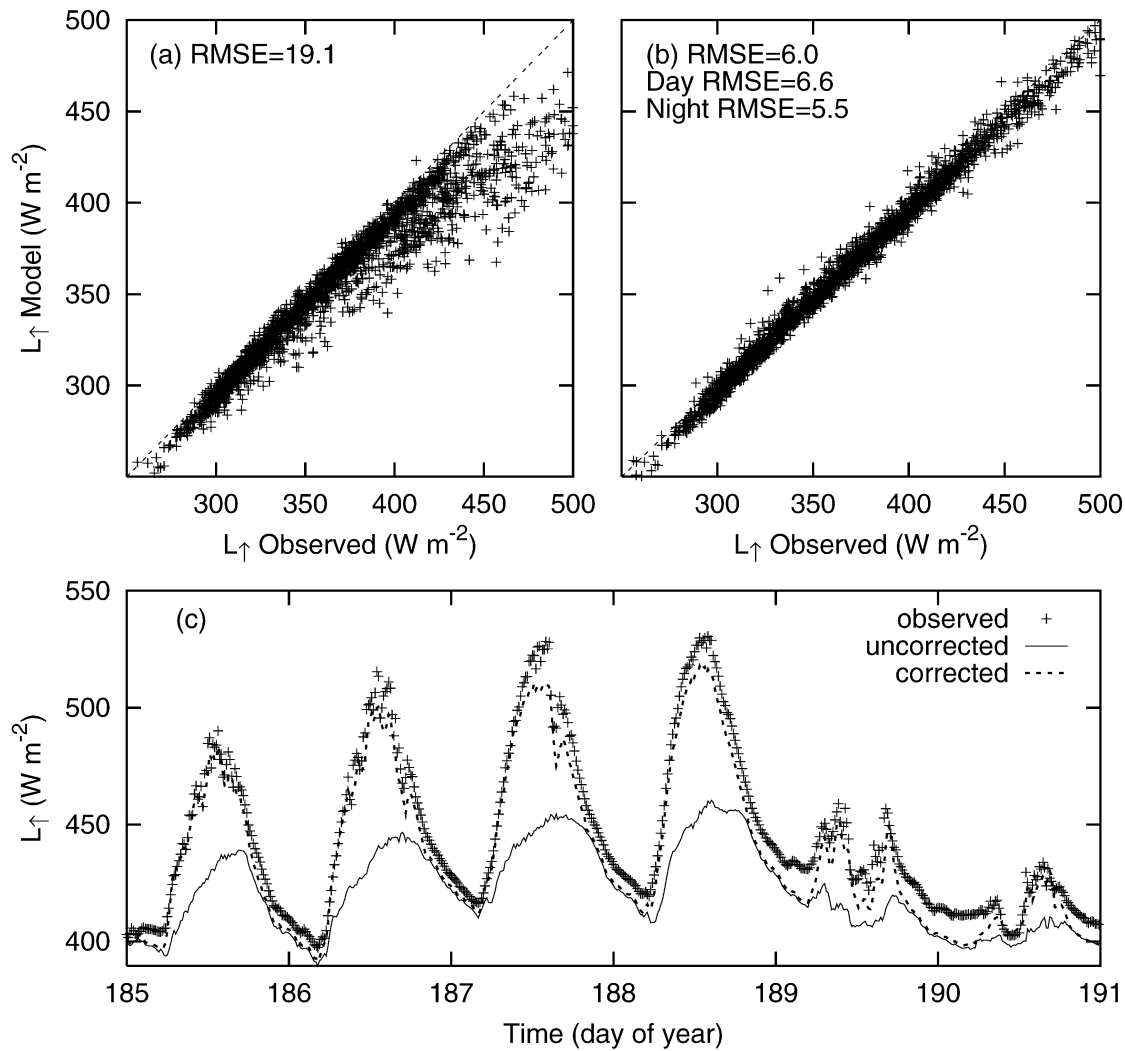
FIG. 7. Similar to Fig. 6 but for $L_\uparrow$. No data were used for function estimation. In (c) partial time series of observations, $L_\uparrow$ with no emissivity correction for cloud, that is, based on (13), and $L_\uparrow$ with emissivity correction for clouds based on (14). In (a) and (b) not all points are shown.

scheme, using all the daytime observations at the three sites. The errors in NARP are predominantly <25 W m^{-2} at each site. The OLS model has a flatter but skewed distribution, so that NARP has the advantage of a greater number of smaller errors.

2) NIGHTTIME RESULTS

In general, errors in the nighttime results are expected to be larger than by day, relative to the magnitude of Q^*, especially because the model is given no infor-

TABLE 4. Performance of NARP (W m^{-2}). Values for Q^* are mean of observations. See text for definition of case 1 and case 2.

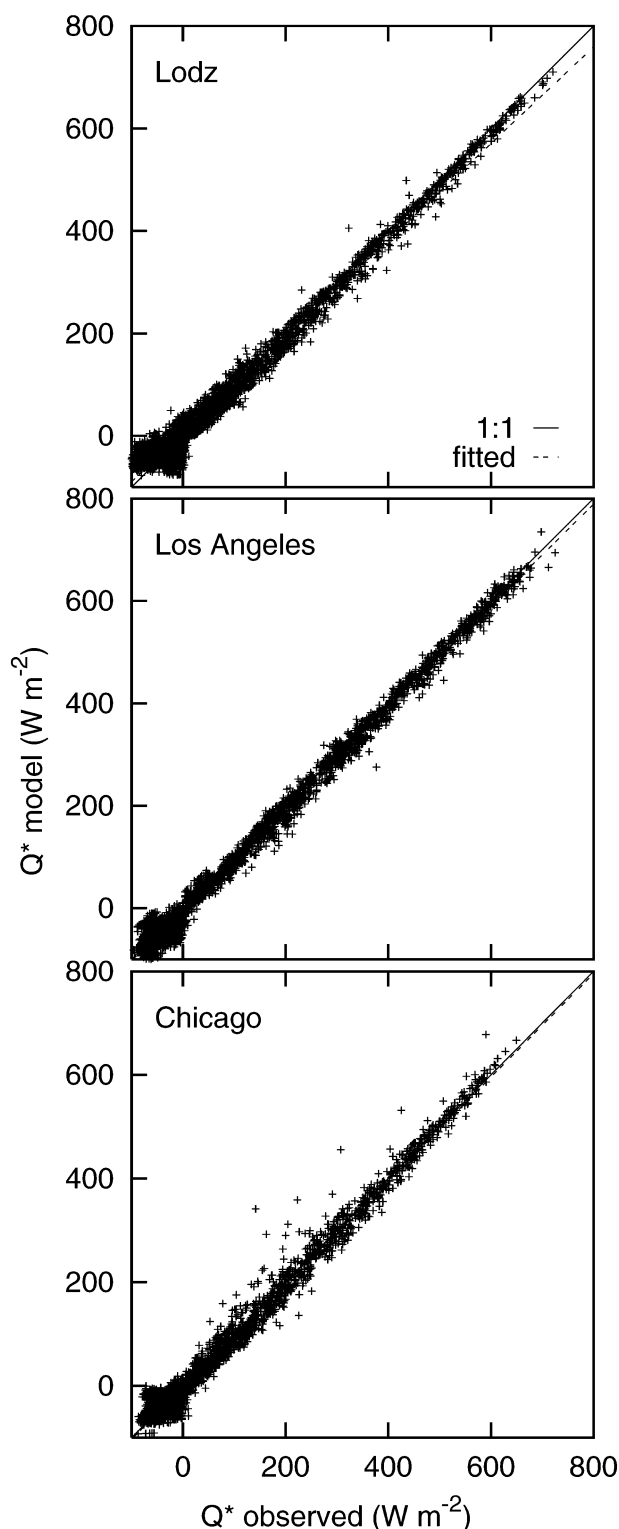|				Day				Night			
				Case 1		Case 2					
Site	Period	N	Q^*	MBE	Rmse	MBE	Rmse	N	Q^*	MBE	Rmse
Łódź	Summer	7515	218	−1.1	19.5	−0.8	19.5	4388	−56	17.2	25.2
	Winter	9289	92	−1.4	22.0	−4.3	21.6	13 847	−34	2.1	28.0
Los Angeles	Summer	5341	292	−31.0	41.0	−6.1	17.2	3930	−43	3.4	20.8
	Winter	9782	205	−12.2	22.1	−4.4	15.6	11 185	−49	−6.3	20.1
Chicago	Summer	4418	204	4.9	18.5	−2.0	16.0	3174	−42	3.5	15.0
	Winter	9987	122	2.8	29.9	−3.9	21.8	12 730	−30	−5.4	19.6

FIG. 8. Modeled (case 2) vs observed Q^* for (top) Łódź, (middle) Los Angeles, and (bottom) Chicago.

mation on cloud cover or surface temperature. Because albedo changes affect the nighttime results only very slightly (because of how night is specified), only case 1 is shown in Table 4. The rmse range from 15 to 28 W m^{-2}, approximately the same range as daytime errors, but are quite large relative to Q^* (81% for Łódź winter). This is attributable mainly to the lack of a good nocturnal cloud estimate. Because of the bias in F_{CLD} at sunset, the MBE is expected to be positive. This is true for Łódź, both for summer and winter, though less pronounced in winter, but only during summer for Chicago and Los Angeles. As noted in section 3a, the Chicago and Los Angeles sites can be expected to have more negative MBE relative to Łódź, and the results are consistent with this expectation. For all sites, the winter period MBE becomes more negative. This can be attributed to fewer clear nights over the winter period (reducing the F_{CLD}-induced bias) and to more neutral (less stable) surface layers. Thus, it seems that even for the less urbanized site, assuming $T_a = T_0$ at night has only a small impact. Although cloud-bias effects could possibly be corrected by making empirical changes to the F_{CLD} formulation, the rmse is largely unsystematic (Fig. 8). Accounting for the nighttime variability in $L_\downarrow$, based on commonly available surface meteorological observations, presents a considerable challenge.

3) TEB ISBA RESULTS

The results from the TEB ISBA scheme were not substantially biased by the chosen site parameters, as was suggested by the difference between estimated and observed albedo (section 3b). The model results (rmse; Table 5) are good when compared with NARP results, as calculated above (Table 4). However, most of this improvement in performance comes from the use of observed $L_\downarrow$ in TEB ISBA ($L_\downarrow$ is the term with greatest error in NARP). When observed values for $L_\downarrow$ are applied to NARP, there is little difference in the performance of the two models (see rmse; Table 5).

Although it seems that NARP does slightly better overall, this only points to the difficulties in constructing correct parameterizations; it does not necessarily suggest that the simpler NARP will perform better in all circumstances. Several factors here are important. First, the treatment of multiple reflections in the generalized urban canyon submodel in TEB allow for a physically based computation of effective albedo and emissivity. NARP used measured albedo, and the same effective emissivity as TEB, so that overall they were probably better estimates. Second, TEB computes the surface energy balance and, therefore, could be expected to produce better estimates of outgoing longwave radiation given the best-case parameterization. However, the smaller errors for NARP at night suggest that air temperature is nearly in equilibrium with the effective surface temperature at this site, also mitigating this advantage. As noted in section 2b(3), highly urbanized set-
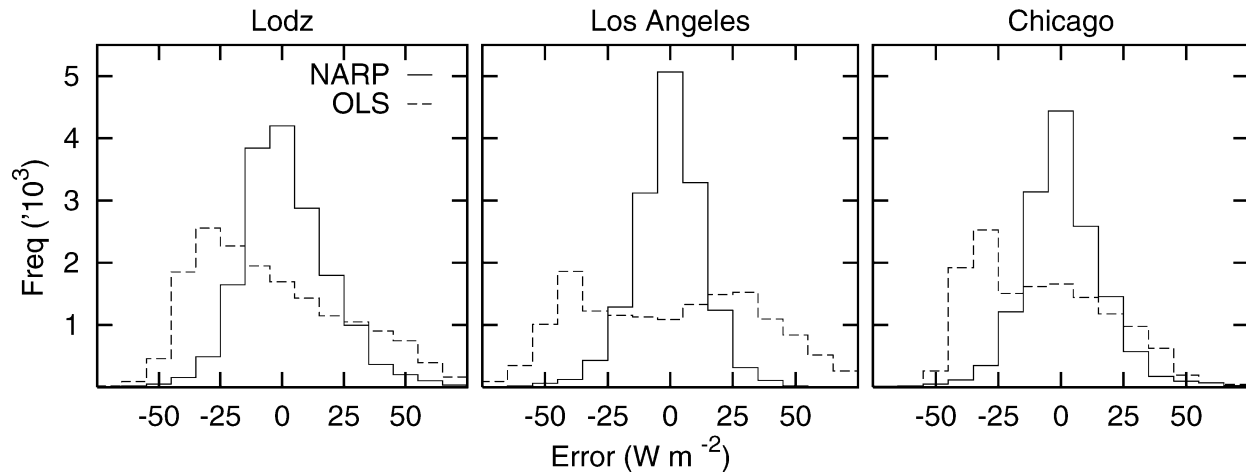
FIG. 9. Histograms of errors (in 10 W m^{-2} bins) incurred by the NARP and OLS models in calculating $Q*$ for (left) Łódź, (middle) Los Angeles, and (right) Chicago (daytime only).

tings have significant nocturnal heat islands that tend to maintain close to a neutral profile through much of the evening and night. Thus, for highly urbanized settings, trying to estimate surface layer outgoing longwave radiation from modeled surface temperatures is inherently more difficult and possibly less accurate in the long run.

d. Sensitivity to inputs and instrument errors

This study raises a number of issues with respect to measuring and modeling $Q*$ near the urban surface. These concerns can be examined by considering the sensitivity of results to potential bias in the inputs, whether due to location or measurement errors. For example, the inputs may not be observed at the same location as the intended value for $Q*$. There may be a vertical, but more frequently horizontal, displacement in space. The following ranges of instrument/location error were considered: T_a, $\pm 3°C$; RH, $\pm 10\%$; $K_\downarrow$, $\pm 5\%$. These were applied to each input variable in separate runs of the model using the same constraints as case 1. The results in terms of MBE are shown in Fig. 10. The model is not strongly affected within this range of T_a or RH, which only affect the longwave results. For a 5% change in $K_\downarrow$, however, the resulting change in MBE is greater than 5%, and this does not consider the like-lihood that a horizontally displaced $K_\downarrow$ observation is also likely to be affected by spatial differences in cloud cover. Perhaps more instructive are the changes in rmse resulting from these changes in inputs shown in Fig. 11. Also shown in Fig. 11 are the results of having a bias of $\pm 5\%$ in the measurement of $Q*$ (note that a negative change is an improvement). Because the Los Angeles site had the worst daytime results for case 1, the effects are larger. Clearly the effects of a bias in either $K_\downarrow$ or $Q*$ have large effects on the model results, up to 32% in the case of Los Angeles. However, because the changes in $Q*$ are similar to the opposite change in $K_\downarrow$, this could be accounted for by a change in albedo. Thus, though sensitive to accuracy in $K_\downarrow$ and $Q*$, assuming unbiased measurements and accurate estimates of albedo, the range of errors for case 2, should be valid for other sites.

5. Conclusions

The performance of a parameterization scheme for net all-wave radiation (NARP) is evaluated using year-long datasets for three urban sites. The parameterization models $Q*$ using as inputs commonly available meteorological fields and basic information about the albedo and emissivity of the surface. Median annual albedo

TABLE 5. Comparison of $Q*$ estimates for Łódź using TEB ISBA and NARP. Note that in this comparison both models are forced using observed $L_\downarrow$ and $K_\downarrow$. All units are watts per meter squared.

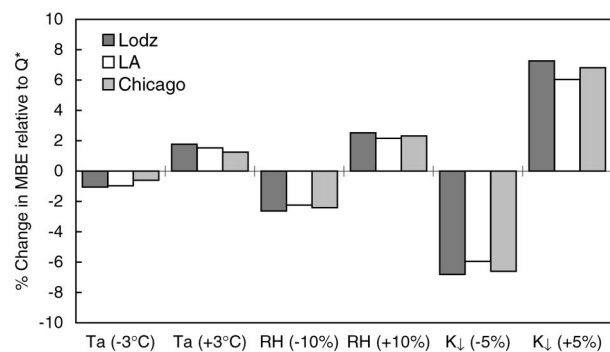|	Mean		TEB ISBA		NARP	
	N	$Q*$	MBE	Rmse	MBE	Rmse
Summer, day	7515	218	−1.6	8.4	8.1	10.2
Summer, night	4388	−56	7.4	7.9	6.4	7.1
Winter, day	9289	92	3.5	14.1	4.7	12.6
Winter, night	13 847	−34	1.6	5.4	3.5	5.0
All	35 039	51	2.2	9.4	5.2	9.0

FIG. 10. Sensitivity of NARP $Q*$ to changes in meteorological inputs for the three sites. Change in input fields are denoted in parentheses.

across sites ranged from 0.08 to 0.21, with the lowest value corresponding to the most densely built site. Seasonal variations were about 20% of the median value, not including snow effects. At the highly urbanized site, seasonal variations were not as important. Thus, choosing a single albedo for all urban sites (i.e., irrespective of degree of urban development) at all times of the year leads to inaccuracies, particularly when substantial amounts of above-building vegetation are present. In comparison with the seasonal changes, incorporating the diurnal variability in albedo has little overall effect. Insufficient data were available here to develop and evaluate a model that includes both effects.

The efficacy of a simple scheme to calculate $L_\uparrow$ with a ''corrected'' near-surface air temperature in place of a true surface temperature was also demonstrated. It was found unnecessary to make nighttime corrections to account for $T_0 - T_a$ differences at the most urbanized site. Cloud impacts on daytime $L_\downarrow$ were incorporated using a method that relies on the notion that cloud effects on

solar transmittance can form the basis of a surrogate parameter in the longwave region.

The results of the NARP for urban sites are better than those achieved by regression models and are comparable to the TEB ISBA model that uses the same number of meteorological inputs and an urban canyon representation but requires specification of more surface and subsurface properties. Both daytime and nighttime $L_\downarrow$ continue to be the largest sources of error in estimating $Q*$ when using only near-surface inputs. In particular, the effects of clouds on longwave radiation exchange are handled poorly. At present, no estimates of nocturnal cloud are included and there is no explicit recognition of cloud height (type).

REFERENCES

Arnfield, A. J., 1982: An approach to the estimation of the surface radiative properties and radiation budgets of cities. *Phys. Geogr.,* **3,** 97–122.

ASHRAE, 1981: *ASHRAE Handbook 1981 Fundamentals.* ASHRAE, 797 pp.

Badescu, V., 1997: Verification of some very simple clear and cloudy sky models to evaluate global solar irradiance. *Sol. Energy,* **61,** 251–264.

Barr, S., and D. L. Sisterson, 2000: Locale analysis report for the Southern Great Plains. U.S. Department of Energy Atmospheric Radiation Measurement Program Tech. Rep. ARM-00-001, 66 pp. [Available online at http://www.arm.gov/docs/sites/sgp/documents/arm00001.pdf.]

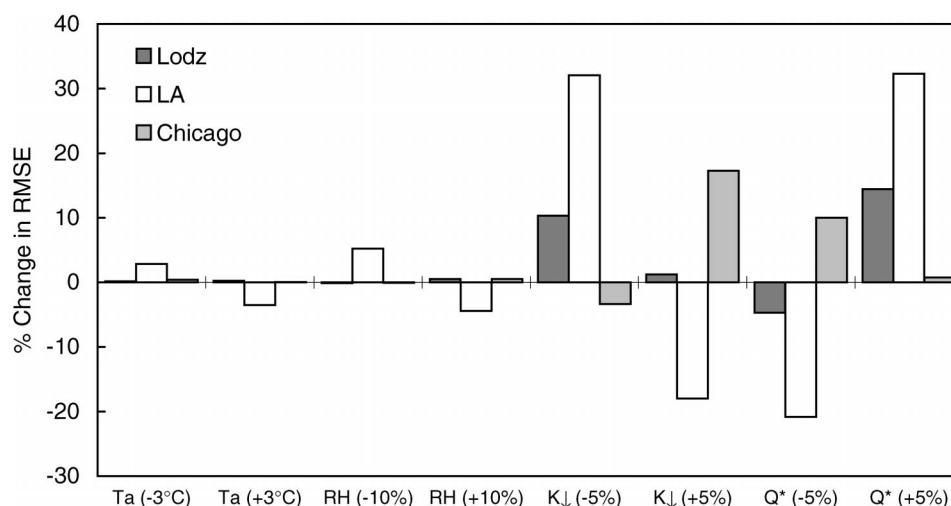Battles, F. J., F. J. Olmo, J. Tovar, and L. Alados-Arboledas, 2000:

FIG. 11. Sensitivity of NARP rmse to changes in all fields for the three sites. Note that a negative change is an improvement. Change in fields are denoted in parentheses.

Comparison of cloudless sky parameterizations of solar irradiance at various Spanish midlatitude locations. *Theor. Appl. Climatol.,* **66,** 81–93.

Brest, C. L., 1987: Seasonal albedo of an urban/rural landscape from satellite observations. *J. Climate Appl. Meteor.,* **26,** 1169–1187.

Climate Prediction Center, 1999: *NOAA/NESDIS and CPC Northern Hemisphere Snow Cover Data.* [Available online at http://www.cpc.ncep.noaa.gov/data/snow/.]

Crawford, T. M., and C. E. Duchon, 1999: An improved parameterization for estimating effective atmospheric emissivity for use in calculating daytime downwelling longwave radiation. *J. Appl. Meteor.,* **38,** 474–480.

De Rooy, W. C., and A. A. M. Holtslag, 1999: Estimation of surface radiation and energy flux densities from single-level weather data. *J. Appl. Meteor.,* **38,** 526–540.

Duchon, C. E., and G. E. Wilk, 1994: Field comparisons of direct and component measurements of net radiation under clear skies. *J. Appl. Meteor.,* **33,** 245–251.

Grimmond, C. S. B., and T. R. Oke, 1999: Aerodynamic properties of urban areas derived from analysis of surface form. *J. Appl. Meteor.,* **38,** 1262–1292.

——, and ——, 2002: Turbulent heat fluxes in urban areas: Observations and a local-scale urban meteorological parameterization scheme (LUMPS). *J. Appl. Meteor.,* **41,** 792–810.

——, C. Souch, and M. D. Hubble, 1996: Influence of tree cover on summertime surface energy balance fluxes, San Gabriel Valley, Los Angeles. *Climate Res.,* **6,** 45–57.

——, ——, R. H. Grant, and G. Heisler, 1994: Local scale energy and water exchanges in a Chicago neighborhood. *Chicago's Urban Forest Ecosystem: Results of the Chicago Urban Forest Climate Project,* E. G. McPherson, D. J. Nowak, and R. A. Rowntree, Eds., USDA Forest Service Northeastern Forest Experiment Station, General Tech. Rep. NE-186, 41–61.

Hodges, E. B., and E. A. Smith, 1997: Intercalibration, objective analysis, intercomparison, and synthesis of BOREAS surface net radiation measurements. *J. Geophys. Res.,* **102,** 28 885–28 900.

Holtslag, A. A. M., and A. P. van Ulden, 1983: A simple scheme for daytime estimates of the surface fluxes from routine weather data. *J. Climate Appl. Meteor.,* **22,** 517–529.

Idso, S. D., D. G. Baker, and B. L. Blad, 1969: Relations of radiation fluxes over natural surfaces. *Quart. J. Roy. Meteor. Soc.,* **95,** 244–257.

Iziomon, M. G., H. Mayer, and A. Matzarakis, 2000: Empirical models for estimating net radiative flux: A case study for three midlatitude sites with orographic variability. *Astrophys. Space Sci.,* **273,** 313–330.

Kaminsky, K. Z., and R. Dubayah, 1997: Estimation of surface net radiation in the boreal forest and northern prairie from shortwave flux measurements. *J. Geophys. Res.,* **102,** 29 707–29 716.

Kipp and Zonen, 2001: Instruction manual CNR1 net-radiometer. 46 pp. [Available from Kipp and Zonen BV, P.O. Box 507, Röntgenweg 1, Delft, Netherlands.]

LI-COR, 1991: LI-COR Terrestrial Radiation Sensor, Type SZ instruction manual. 24 pp. [Available from LI-COR, P.O. Box 4425, Lincoln, Nebraska.]

Masson, V., 2000: A physically-based scheme for the urban energy balance in atmospheric models. *Bound.-Layer Meteor.,* **94,** 357–397.

——, C. S. B. Grimmond, and T. R. Oke, 2002: Evaluation of the Town energy balance (TEB) scheme with direct measurements from dry districts in two cities. *J. Appl. Meteor.,* **41,** 1011–1026.

Meyn, S. K., 2000: Heat fluxes through roofs and their relevance to estimates of urban heat storage. M.S. thesis, Dept. of Geography, University of British Columbia, Vancouver, BC, Canada, 106 pp. [Available from T. Oke at toke@geog.ubc.ca.]

Newton, T., 1999: Energy balance fluxes in a subtropical city: Miami, FL. M.S. thesis, Dept. of Geography, University of British Columbia, Vancouver, BC, Canada, 140 pp. [Available from T. Oke at toke@geog.ubc.ca.]

Niemelä, S. P., P. Räisänen, and H. Savijärvi, 2001a: Comparison of surface radiative flux parameterizations. Part I: Longwave radiation. *Atmos. Res.,* **58,** 1–18.

——, ——, and ——, 2001b: Comparison of surface radiative flux parameterizations. Part II: Shortwave radiation. *Atmos. Res.,* **58,** 141–154.

Noilhan, J., and S. Planton, 1989: A simple parameterization of land surface processes for meteorological models. *Mon. Wea. Rev.,* **117,** 536–549.

Offerle, B., C. S. B. Grimmond, K. Fortuniak, T. R. Oke, and K. Klysik, 2002: Analysis of long-term observations of urban surface-atmosphere energy exchange. Preprints, *Fourth Symp. on the Urban Environment,* Norfolk, VA, Amer. Meteor. Soc., 103–104.

Oke, T. R., 1987: *Boundary Layer Climates.* Routledge, 435 pp.

——, 1988: The urban energy balance. *Progr. Phys. Geogr.,* **12,** 471–508.

——, 1995: The heat island of the urban boundary layer: Characteristics, causes and effects. *Wind Climate in Cities,* J. E. Cermak et al., Eds., Kluwer Academic, 81–107.

Oncley, S. P., and Coauthors, 2002: The energy balance experiment EBEX-2000. Preprints, *25th Conf. on Agricultural and Forest Meteorology,* Norfolk, VA, Amer. Meteor. Soc., 1–2.

Paltridge, G. W., and C. M. R. Platt, 1976: *Radiative Processes in Meteorology and Climatology.* Elsevier Scientific, 318 pp.

Prata, A. J., 1996: A new long-wave formula for estimating downward clear-sky radiation at the surface. *Quart. J. Roy. Meteor. Soc.,* **122,** 1127–1151.

Roth, M., 2000: Review of atmospheric turbulence over cities. *Quart. J. Roy. Meteor. Soc.,* **126,** 941–990.

Sailor, D. J., and H. Fan, 2002: Modeling the diurnal variability of effective albedo for cities. *Atmos. Environ.,* **36,** 713–725.

Schmid, H. P., H. A. Cleugh, C. S. B. Grimmond, and T. R. Oke, 1991: Spatial variability of energy fluxes in suburban terrain. *Bound.-Layer Meteor.,* **54,** 249–276.

Sellers, W. D., 1965: *Physical Climatology.* The University of Chicago Press, 272 pp.

Smith, W. L., 1966: Note on the relation between total precipitable water and surface dew point. *J. Appl. Meteor.,* **5,** 726–727.

Sozzi, R., A. Salcido, R. Saldaña Flores, and T. Georgiadis, 1999: Daytime net radiation parameterization for Mexico City suburban areas. *Atmos. Res.,* **50,** 53–68.

Sugita, M., and W. Brutsaert, 1993: Cloud effect in the estimation of instantaneous downward longwave radiation. *Water Resour. Res.,* **29,** 599–605.

USEPA, 1999: PCRAMMET User's Guide. U.S. Environmental Protection Agency, Office of Air Quality Planning and Standards, Emissions, Monitoring, and Analysis Division, Tech. Rep. EPA-454/B-96-001 95 pp. [Available online at http://www.epa.gov/scram001/userg/relat/pcramtd.pdf.]

van Ulden, A. P., and A. A. M. Holtslag, 1985: Estimation of atmospheric boundary layer parameters for diffusion applications. *J. Climate Appl. Meteor.,* **24,** 1196–1207.